A study of orientation spin vector of g- magnitude of SDSS DR-13 galaxies having redshift 0.50 to 0.53

Rabina Kadariya*, Prabin Karki, Birendra Prasad Yadav*** and Shiv Narayan Yadav*****

*Patan Multiple Campus, T. U, Lalitpur,

**Department of Physics and Astronomy, University of Wisconsin Milwaukee, USA

***Central Department of Physics, TU, Kirtipur

Abstract: With a focus on galaxies with redshifts between 0.50 and 0.53 we have studied the spatial alignment of 106,019 galaxies surveyed by the Sloan Digital Sky Survey (SDSS). The SDSS telescope in New Mexico USA was equipped with a 447 nm Charged Coupled Device (CCD) filter to record the g-magnitudes. We transformed two-dimensional given constraints into three-dimensional parameters, polar and azimuthal angle. In order to ascertain the theoretical isotropic distribution of galaxy rotation axes while taking into account different selection effects we conducted random simulations by creating 10^7 virtual galaxies using the methodology described by earlier studies. Chi-square, autocorrelation, and Fourier analysis were the three statistical tests we used to examine the differences between the theoretical and observed distributions. The main goals are to investigate non-random effects in galaxy orientations and evaluate how well the selected coordinate system explains the actual orientation of far-off galaxies. Our results show that the spin vectors in samples g01, g02, g05, and g06 have an isotropic distribution which is consistent with the Hierarchy Model of galaxy evolution. The reference coordinate system is the cause of the controversy for few samples. Additionally, g07 has a significant negative value consistent with the Primordial Vorticity Model while go3 and go4 have significant positive first order Fourier coefficients supporting the Pancake model.

Keywords: Galaxies; Orientations; Angular momentum; Hierarchy.

Introduction

The universe started out with the huge Bang about 13.8 billion years ago. For the primary tiny fraction of a second after big bang all four forces are in fundamental symmetric and consequently activities within 10^{-43}s are beyond physics. The foremost points can be defined as follows: from beginning to about 10^{-6} seconds of big bang particle physics rules. After 1 second, subatomic debris had been shaped and after 360,000 years belongings have cooled down sufficient in order that normal factors like hydrogen should exist [1-2]. the amount of hydrogen in the universe these days is one of the important portions of proof for the huge bang. Density fluctuations in the early Universe had been exponentially amplified all through a segment of inflation [3], a theory that removes a number of the problems so known as general big bang model. According to von Weizscker [4] the observed angular momentum distributions of galaxies are important for cosmology and galaxies rotation might be a clue of physical conditions beneath which those structures shaped. For this reason, the distribution of spatial orientations of the spin vectors can supply the starting place of angular momenta of galaxies. Peebles [5] confirmed that the angular momentum of rotation of the galaxy has the same opinion in value with the prediction of the cosmological imbalance for the galaxy formation. Our images is a try to work out a choice to this type of theories. The concept in the back of is statistical research of the spin vectors of the galaxies. That is a excellent method, due to the fact the theory predicts

Author for correspondence: Shiv Narayan Yadav, Central Department of Physics, T. U, Kirtipur, Kathmandu Nepal.
Email: shiva.yadav@cdp.tu.edu.np; https://orchid.org/0009-0005-5486-0158
Received: 19 Apr, 2026: Received in revised form: 9 May, 2026; Accepted: 16 May, 2026.
Doi: https://doi.org/10.3126/sw.v19i19.95712

exceptional alignments of these vectors, which can be used as a criterion. So, the purpose is to evaluate observational facts with predictions from the theories [6]. The current advancement in technology has supplied us with the huge quantity of facts of the numerous galaxies, clusters and superclusters in the universe, a right evaluation and interpretation of such facts with right computation of the to be had facts can assist us find the distribution of the angular momentum vector of galaxies in the cluster and Supercluster which might be useful to recognize the early levels of the formation of galaxies and clusters supplied that the angular momentum of galaxies has now not changed drastically [7-20]. A comparative and analytical take a look at of the favored alignment of the spin vectors of galaxies (SDSS) in the COMA cluster the use of the position angle inclination method [21] with appreciate to equatorial coordinate system (ECS), Galactic coordinate system (GCS) and exceptional galactic coordinate system (SGCS) can supply statistics about the evolution of the COMA [22].

Models for galaxy evolution

Only three of the many theories are based on the direction of the spin vector as will be discussed below.

According to the pancake model [23–24] galaxies angular momentum is predicted to be parallel to the reference plane. This model states that clusters formed first and then broke up into galaxies as a result of adiabatic fluctuations. According to the non-linear theory of gravitational instability thin dense gaseous condensations known as pancakes are created when tiny inhomogeneities grow. The hierarchy model [5] states that galaxies angular momentum should be aligned haphazardly. According to the model galaxies were first created and as they gathered gravitationally to form clusters the tidal force gave them their angular momenta. These galaxies develop through the consequent integration of protogalactic condensation or even through the merging of galaxies that have already reached full formation [25].

According to the primordial vorticity theory [26–28] the angular momentum is perpendicular to their plane of coordinate system. Galaxies were formed as a result of density and pressure fluctuations in the early universe

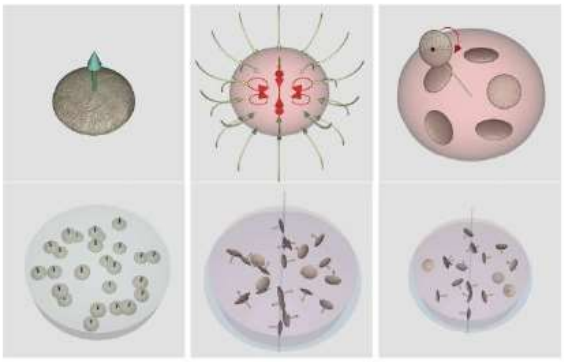

Figure 1: Explanation of the spatial orientations of angular momentum vectors of galaxies based on three existing models: primordial vorticity, pancake and hierarchy model. An arrow represents the preferred direction of the angular momentum vector of a galaxy in each model [29].

which is known as primordial vorticity. It is also known as a top-down scenario.

Godlowskian transformation

The polar angle (θ) and the azimuthal angle (Φ) are the variables that define the direction of the angular momentum of galaxies. The comprehensive derivations of the expressions for the angles θ and Φ are presented in [21]. Using the equatorial coordinate system as a reference, θ and Φ can be derived from measurable quantities in the following way:

$$\sin\theta = -cosi\ sin\alpha \pm sini\ sinPcos\delta \quad (1)$$

$$\sin\phi = (\cos\theta)^{-1}\left[-\cos i\cos\delta\sin\alpha + \sin i\left(\frac{\mp\sin P\sin\delta\sin\alpha\mp}{\cos P\cos\alpha}\right)\right] \quad (2)$$

where i represents the inclination angle, defined as the angle between the normal to the galaxy plane and the observer's line of sight. The angle of inclination can be calculated using the formula [26]

$$\cos^2 i = \frac{(q^2 - q^{*2})}{(1-q^{*2})} \quad (3)$$

Here, q is axial ratio (b/a) and q^* be the intrinsic flatness of the galaxy, respectively. Here, α, P, and δ be the right ascension, position angle and declination of the galaxies.

Method of analysis

Aryal and Saurer [14] came to the conclusion that any database selections could significantly alter the expected isotropic distribution curves shapes and virtual galaxies

should emerge to compensate for this flaw. To describe expected distribution curves for θ and ϕ simulations are run using equations (1, 2). The isotropic distribution curve is derived from 10^7 virtual galaxies simulations. Initially the distributions of α, δ, P and i are observed for the galaxies in our samples and distributed using 10^7 virtual galaxies for the corresponding parameters [12]. Using MATLAB 2015a these numbers are used to create an input file and the expected distribution.

The isotropic curves in both θ and ϕ are compared with our observations (real observed dataset). Three distinct statistical tests are employed for this comparison: the chi-square, Fourier and auto correlation tests.

Chi-square test.

The chi-square test is an impartial approach to ascertain if the observed distribution deviates from the anticipated distribution specified by. It assesses the compatibility of a theoretical probability distribution with a given data set

$$\chi_\nu^2 = \frac{\chi^2}{\nu} \qquad (4)$$

and $\boldsymbol{\chi^2} = \sum_{i=1}^{n} \frac{(N_{0i}-N_{ei})^2}{N_{ei}}$ (5)

Here, n, N_{0i} and N_{ei} represent bins, the observed and expected distributions and $\nu = n$-1 be the degree of freedom.

Fourier test

The expressions for the Fourier coefficients Δ_{11} and Δ_{21} are [30]

$$\Delta_{11} = \frac{\sum_{k=1}^{n}(N_k - N_{0k})\cos 2\theta_k}{\sum_{k=1}^{n} N_{0k}\cos^2 2\theta_k}$$
$$\Delta_{21} = \frac{\sum_{k=1}^{n}(N_k - N_{0k})\sin 2\theta_k}{\sum_{k=1}^{n} N_{0k}\sin^2 2\theta_k} \qquad (6)$$

The standard deviations $\sigma(\Delta_{11})$ and $\sigma(\Delta_{11})$ can be obtained using the expressions equation 7.

Let, $\Delta_1 = \left(\Delta_{11}{}^2 + \Delta_{21}{}^2\right)^{1/2}$ is amplitude of the Fourier

$$\sigma(\Delta_{11}) = \left(\sum_{k=1}^{n} N_{0k}\cos^2 2\theta_k\right)^{-1/2}$$
$$\sigma(\Delta_{21}) = \left(\sum_{k=1}^{n} N_{0k}\sin^2 2\theta_k\right)^{-1/2} \qquad (7)$$

coefficient and the first-order Fourier probability can be calculated by formula

$$P(>\Delta_1) = exp\left(-\frac{n}{4}N_0\Delta_1{}^2\right)$$

Auto correlation test

The auto-correlation test assesses the extent of a linear relationship between two variables. In our scenario, it considers the relationship between the quantity of galaxies in neighboring angular bins. The correlation function is referenced in [31]

$$C = \sum_{1}^{n} \frac{(N_k - N_{0k})(N_{k+1} - N_{0k+1})}{(N_{0k}N_{0k+1})^{1/2}} \qquad (8)$$

and

$$\sigma(C) = (n)^{1/2}$$

Results & Discussion

The thresholds for anisotropic are P (> χ2) < 0.050, (C/C(σ)) > 1.0, ($\Delta_{11}/\sigma(\Delta_{11})$) > 1.5, and P(> Δ_1) < 0.150. The distributions of the polar and azimuthal angles are accessible in Table 1 and Table 2. The notable -ve value of $\Delta_{11}/\sigma(\Delta_{11})$ for θ shows that angular momentum are likely aligned perpendicularly, while a +ve value advises they are aligned parallel to the reference plane. In the statistical analysis of ϕ, a positive notable value of $\Delta_{11}/\sigma(\Delta_{11})$ specifies that the projections of spin of galaxies are inclined toward the center, while a prominent negative value of ($\Delta_{11}/\sigma(\Delta_{11})$) signifies align tangentially [32].

A hump (or dip) in the smaller θ ((0°< θ < 45°).) indicates that the spin vectors of galaxies are likely to align parallel (or perpendicular) to the equatorial coordinate system. Likewise, a peak (or trough) in the larger θ suggests that the spin vectors of galaxies are generally aligned perpendicular to the reference coordinate system [33].

In the histogram of the ϕ-distribution, the solid circles with

±1σ error bars also depict the observed distribution. The peaks and dips in the ϕ-distribution histograms are more challenging to interpret than those of θ-distributions [34-35]. This is due to the fact that the range of ϕ spans from -90º to +90º.

Table 1: The first, second, third and fourth columns indicates name of sample, chi-square probability, Auto-correlation coefficient and the first order Fourier coefficient respectively and last column denotes Fourier probability of θ.

Sample	P(> χ2)	C/σ(C)	$\Delta_{11}/\sigma(\Delta_{11})$	P(Δ_1)
g01	0.120	−1.0	0.3	0.940
g02	0.060	−1.0	−0.6	0.466
g03	0.002	4.7	3.6	0.005
g04	0.037	4.3	3.2	0.004
g05	0.399	−0.4	−0.5	0.465
g06	0.008	0.4	−1.3	0.002
g07	0.019	1.9	−2.0	0.012

.

Table 2: The first, second, third and fourth columns indicates name of sample, chi-square probability, Auto-correlation coefficient and the first order Fourier coefficient respectively and last column denotes Fourier probability of ϕ.

Sample	P(>χ2)	C/C(σ)	$\Delta_{11}/\sigma(\Delta_{11})$	P(>Δ_1)
g01	0.052	1.0	0.7	0.240
g02	0.478	−0.1	0.0	0.748
g03	0.007	21.5	10.6	0.009
g04	0.000	19.5	9.9	0.000
g05	0.000	7.8	6.1	0.000
g06	0.047	−0.7	2.0	0.117
g07	0.010	2.0	1.8	0.089

Sample; g01

To begin, we examine the distribution of galaxies in sample g01 concerning θ and ϕ for g-magnitudes between 16.5 and 17.0. The data for the distribution of the polar angle (θ) in this sample is presented in table 1, which indicates P (> χ2) = 0.120, C/σ(C) = -1.0, ($\Delta_{11}/\sigma(\Delta_{11})$) = 0.3, and P(>$\Delta_1$) = 0.940. All of these statistics advocate isotropy [36-38].

In Figure 2, the count of observed galaxies stands at 2,926 while the anticipated solutions total 2,931 for small angles (0°< θ < 40°). In this area, one peak is seen at an angle of 7.5° with >1σ error margin, while three dips are noted at angles of 2.5°, 12.5°, and 17.5° respectively, with <1σ error margin. This dip balanced the hump. In bimodal regions (40° < θ < 50°), there are 521 observed galaxies and 489 expected galaxies, indicating that the observed count exceeds the expected count by 32. Additionally, no notable rises or declines can be seen in this area. For 50° < θ < 90°, the expected and actual number of galaxies are recorded as 857 and 831 respectively. The observed number of galaxies is 26 fewer than the expected number of galaxies. In this case, no notable hump or dip is detected either. We have observed that galaxies are distributed randomly, conforming to the Hierarchy model in the θ distribution [5].

The second row of table 2 presents the statistics for ϕ of sample g01. In this sample, the value of P (>χ2) = 0.060, C/σ (C) = -1.0, ($\Delta_{11}/\sigma(\Delta_{11})$) = 0.7, and P (>$\Delta_1$) = 0.240. All statistics specify isotropy.

In Figure 2, the total galaxies observed and the expected galaxies within ten central bins (φ ~ ±45◦) were 2,869 and 2,769, respectively. In this area, three peaks are noted at angles -25°, -15°, and 25° with < 1σ error margin, while one trough is seen at 5° with < 1σ error margin. Moreover, beyond this area, in the first and final four bins, the observed distributions are 57 lower than anticipated. Two dips at angles of -75° and 75° are noted with an error limit of less than 1σ.

With carefully analysis of the data related to polar and azimuthal angles, we determined that the spin vectors of galaxies exhibit isotropy and are randomly distributed in the g01 sample. This endorses the Hierarchy model of galaxy creation.

Sample; g02

Here, we discuss θ and ϕ distribution of sample g02 for g-magnitudes of range 17.0 to 17.5. The third row of table 1 shows the statistics of θ distribution in sample g02. The P (>χ^2) = 0.060, C/σ (C) = -1.0, $\Delta_{11}/\sigma(\Delta_{11})$ = 0.600 and P (> Δ_1) = 0.466. All these statistics suggest isotropy.

In this section, we examine the θ and ϕ distribution of sample g02 with g-magnitudes varying between 17.0 and 17.5. The P (>χ2) = 0.060, C/σ (C) = -1.0, ($\Delta_{11}/\sigma(\Delta_{11})$) = 0.600, and P (> Δ_1) = 0.466. All these figures imply isotropy. In Figure 3, the count of observed and expected

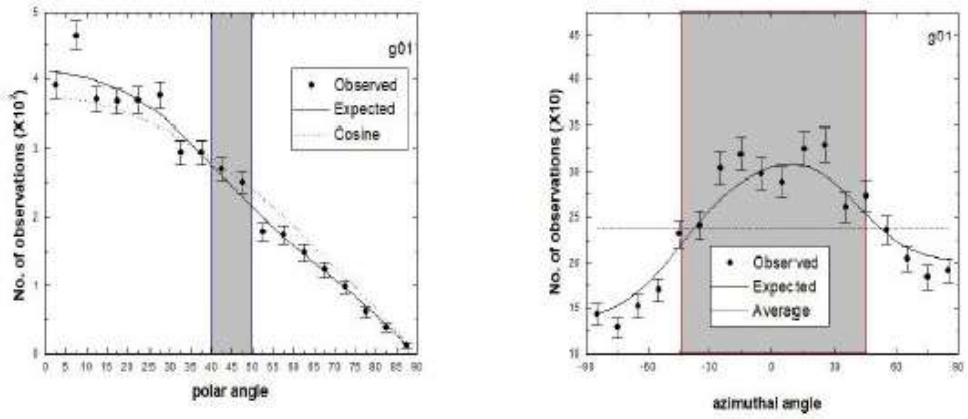

Figure 2: θ and ϕ distributions of SDSS galaxies having g-magnitude. The solid line represents the expected isotropic distributions. The cosine and average distribution (dashed) is shown for the comparison. The statistical error (±1σ) bars on solid circle represent observed distribution.

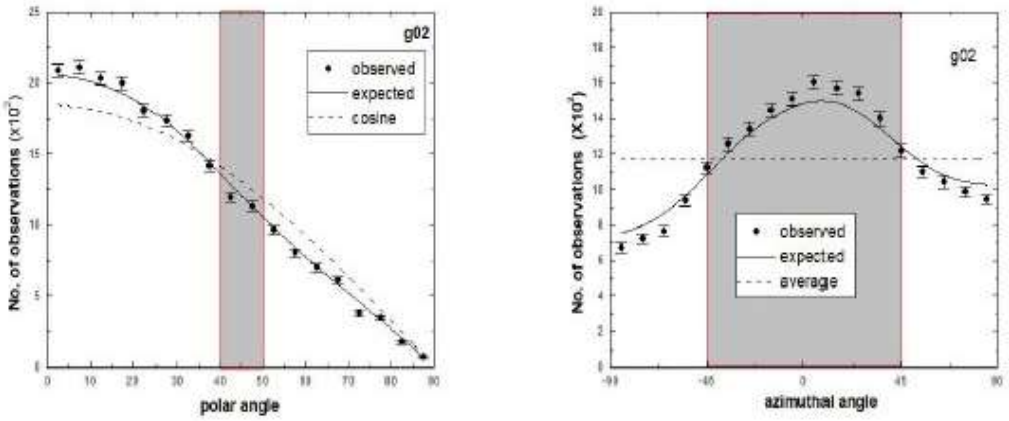

Figure 3: The θ and ϕ distributions of SDSS galaxies having g-magnitude. The solid line represents the expected isotropic distributions. The cosine and average distribution (dashed) is shown for the comparison. The statistical error (±1σ) bars on solid circle represent observed distribution.

distributions stand at 14,802 and 14,612 for small angles ($0° < \theta < 40°$). In this area, two minor peaks are noted at angles of 7.5° and 17.5° with < 1σ error margin. In the bimodal region ($40° < \theta < 50°$), the observed distributions are 2,322 while the expected distributions are 2,404, meaning the expected distributions exceed the observed ones by 82. A small decline is noted at 42.5° with < 1σ error margin in this area. For $50° < \theta < 90°$, the observed and expected number of galaxies are 4,038 and 4,158 respectively, indicating that the observed galaxies are fewer by 107 compared to the expected number. One dip at an angle of 72.5° with an error limit greater than 1σ is identified here.

The second line of table (2) presents the statistics for the azimuthal angle (ϕ) distribution of galaxies in sample g02, where P ($>\chi 2$) = 0.478, C/σ (C) = -0.1, ($\Delta_{11}/\sigma(\Delta_{11})$) = 0.0, and P($>\Delta_1$) = 0.748. These statistics indicate isotropy.

In Figure 3, for ($\varphi \sim \pm 45°$), the counted and anticipated number of galaxies in ten central bins are recorded as 14,001 and 13,508, respectively. In this area, three notable peaks are seen at 5°, 15° and 25° with 1σ error range.

Sample; g03

We examine θ and ϕ for sample g03 with g-magnitude between 17.5 and 18.0. The P ($>\chi 2$) = 0.002, C/σ (C) = 4.7, ($\Delta_{11}/\sigma(\Delta_{11})$) = 3.6, and P ($>\Delta_1$) = 0.005. A positive significant value of the 1st order Fourier coefficient indicates that the spin vectors of galaxies are likely aligned parallel to the equatorial coordinate system. All these figures indicate anisotropy.

In Figure 4, the observed galaxies total 37,599, while the anticipated solutions are 37,281 for small angles ($0° < \theta < 40°$). In this area, two peaks are noted at 12.5° with a 2σ error margin and at 17.5° with a 1σ error margin. In the bimodal region ($40° < \theta < 50°$), the counts for observed and expected galaxies are 6,276 and 6,211 respectively. In this area, neither a hump nor a dip is detected. For $50° < \theta < 90°$, the detected and expected number are 10,345 and 10,726 correspondingly.

The data for the azimuthal angle (ϕ) distribution in sample g03 indicates P ($>\chi 2$) = 0.007, C/σ (C) = 21.5, ($\Delta_{11}/\sigma(\Delta_{11})$) = 10.6, and P ($>\Delta_1$) = 0.009. All these figures indicate significant anisotropy.

In Figure 4, the counted galaxies in ten central bins total 34,867, whereas the predicted count of galaxies is 33,816 for ($\varphi \sim \pm 45^0$). In this area, five peaks are noted at an angle of -35° with 1σ error limit, -5° with 1σ error limit, 5° with > 1σ error limit, 15° with > 1σ error limit, and 25° with > 1σ error limit. In the outer region, the expected distributions in the first four bins exceed the observed distribution by 615. Two dips are noted at -85° with a 1.5σ error margin and at -75° with an error limit of less than 2.5σ. In the last

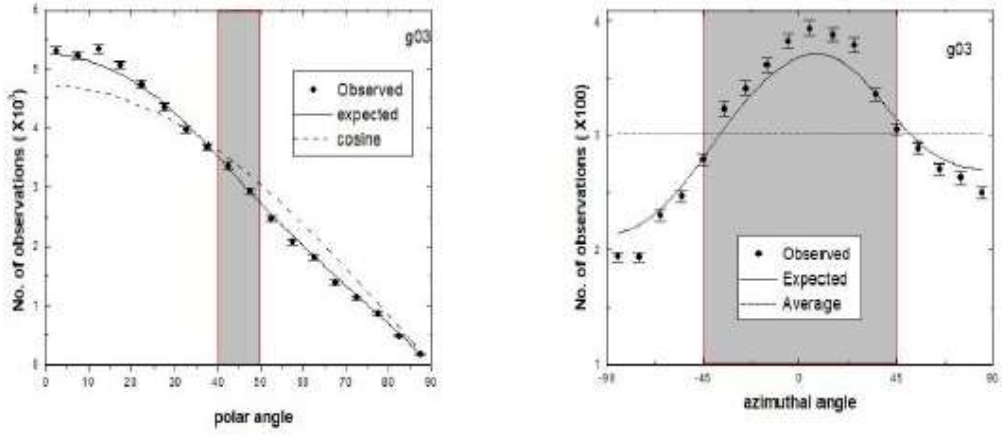

Figure 4: The polar (θ) and azimuthal angle distributions of SDSS galaxies having g-magnitude. The solid line represents the expected isotropic distributions. The cosine and average distribution (dashed) is shown for the comparison. The statistical error (±1σ) bars on solid circle represents observed distribution.

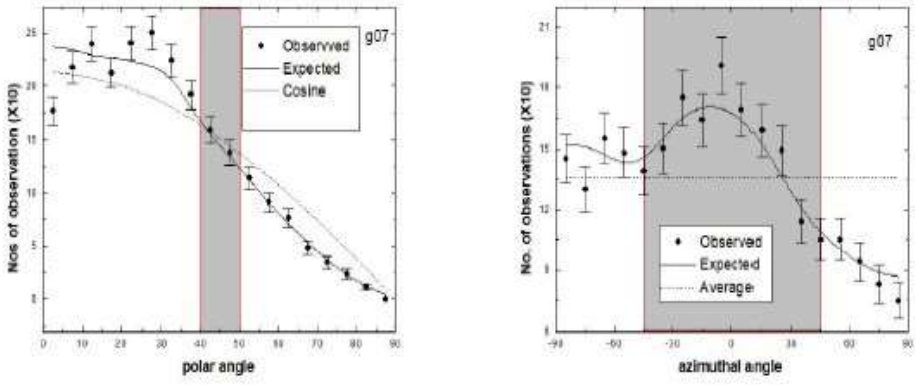

Figure 5: The θ and ϕ distributions of SDSS galaxies having g-magnitude. The solid line represents the expected isotropic distributions. The cosine and average distribution (dashed) is shown for the comparison. The statistical error (±1σ) bars on solid circle represent observed distribution.

four bins, the observed distributions fall short of expectations by 435. We noted two minor dips at angles of 65° and 75° with < 1σ error margin, and one further dip at an angle of 85° with a 2σ error margin. Deep analysis of the statistics and graph regarding polar and azimuthal angles, we observed that the spin vectors of galaxies generally align

parallel to the plane that underpins the Pancake model. Comparable outcomes are observed for samples g04, g05, and g06.

Sample; g07

We analyze θ and ϕ for sample g03 galaxies with g-magnitude between 19.5 and 20.0. The P ($>\chi 2$) = 0.019, C/σ (C) = 1.9, ($\Delta_{11}/\sigma(\Delta_{11})$) = -2.0 and P($>\Delta_1$) = 0.012. A negative significant value of the 1st order Fourier coefficient indicates that the spin vectors of galaxies are generally aligned perpendicularly to the equatorial coordinate system. All these figures indicate anisotropy.

In Figure 5, the detected and expected solutions are 1,756 and 1,762, respectively, for small angles ($0° < \theta < 40°$). In the region, a single hump is noted at 25.5° with less than 1σ error margin, while a significant trough at 2.5° results in anisotropy. In the bimodal region (($40° < \theta < 50°$), the actual solution exceeds the anticipated number by 8. For $50° < \theta < 90°$, the counted and expected galaxies are 397 and 399. In these areas, no notable rises and falls are observed.

The data for the azimuthal angle distribution in sample g07 indicates that the Chi-square probability is 0.010, the Auto-correlation coefficient equals 2.0, the First order Fourier coefficient is 1.8, and the first order Fourier probability is 0.089. Therefore, all data confirms anisotropy. In Figure 5, the actual count of galaxies and the expected count of galaxies in ten central bins are observed to be 1,515 and 1,489 respectively for ($\varphi \sim \pm 45°$). Therefore, the actual count of galaxies exceeds the anticipated number by 26. In this area, a hump at an angle of 5° with less than 1σ error margin is noted. In the outer region, the observed distribution in the first four bins is lower by 14 compared to the expected, while in the last four bins. The observed value is 10 below the expected. A single dip occurs at an angle of -75° with a < 1σ error margin in the initial four bins. In the last four bins, a noticeable decline is observed at an angle of 85° with < 1σ. After careful analysis of the data and plots related to polar and azimuthal angles, we concluded that there is anisotropy and the spin vector perpendicular orientation to the plane. This backs the Primordial Vorticity model for galaxy evolution.

Conclusion

The primary aim of this thesis is to analyze non-random effects within the galaxy and to determine the suitable coordinate system for depicting the actual orientation of distant galaxies. The insights gained from these observations are as follows:

The isotropic distribution of spin vectors and their projections in galaxies from samples g01, g02, g05, and g06 has been observed, re-inforcing the Hierarchy model of galaxy evolution [5].

In samples g03, and g04 a random distribution of spin vectors and their projections for galaxies is observed. Statistical parameters indicate that this sample favors the Pancake model of galaxy evolution [23, 24]. In sample g07, we observed a random distribution of the spin vector and its projections, which aligns with the Primordial Vorticity model [27-29].

No favored arrangement is observed in the spatial alignment of spin vectors in galaxies, indicating a hierarchy model. Nonetheless, a localized impact was noted in the majority of the samples. In these subsamples, a local tidal link between the rotation axes of galaxies or the process of merging is anticipated. Consequently, the angular momentum vector of several galaxies is influenced [36].
The peaks and troughs in the distribution of angular momentum are seen in various subsamples, attributed to the local influence of the galaxy. We anticipated a density variation and detected it on a local scale in the deep field.

We employed equatorial coordinate systems as physical references to examine non-random effects related to galaxy orientation. The hierarchy model suggests that selecting a coordinate system does not change favored alignments. Nonetheless, proponents of the pancake model emphasize the significance of a physical reference system. We discovered a variety of outcomes: in the majority of instances, the hierarchy model, and in a limited number of cases, the pancake model and turbulence model in specific areas. We employed an alternative system like the Galactic or Supergalactic system to tackle this issue [37, 38].

Acknowledgements

The authors would like to thank Department of Physics, Patan Multiple, Campus and Central department of physics, Tribhuvan University, Professor Dr. Narayan Prasad Adhikari, Dr. Kishori Yadav, Mr. Mahesh Kumar Chaudhary and Sloan Digital Sky Surveys (SDSS).

References

[1] Aryal, B. 2002. *Spatial Orientation of Spin Vectors of Galaxies in 42 Abell Clusters*. Ph.D. thesis. Institute of Astro- and Particle Physics, Innsbruck University, Technikstrasse 25/8, A-6020 Innsbruck, Austria.

[2] Aryal, B. 2011. Winding sense of galaxies around the local supercluster. *Research in Astronomy and Astrophysics*. **11**: 293-304. Doi: https://doi.org/10.1088/1674-4527/11/3/004

[3] Gamow, G. 1952. The role of turbulence in the evolution of the universe. *Phys. Rev*. **86**: 251-260. Doi: https://doi.org/10.1103/physrev.86.251

[4] Von Wiezsacker, C. F. 1951. The evolution of galaxies and stars. *The Astrophysical Journal*. **14**: 165-186. Doi: https://doi.org/10.1086/145462

[5] Peebles, P. J. E. 1969. Origin of the angular momentum of galaxies. *The Astrophysical Journal*. 155: 393-401. Doi: https://doi.org/10.1086/149876

[6] Aryal, B., Kandel, S. & Saurer, W. 2006. Spatial orientation of galaxies in the core of the Shapley concentration - the cluster Abell. *Astronomy & Astrophysics*. **458**: 357-367. Doi: https://doi.org/10.1051/0004-6361:20065179

[7] Aryal, B., Paudel, S. & Saurer, W. 2007. Spatial orientations of galaxies in seven Abell clusters of BM type II. *Monthly Notices of the Royal Astronomical Society*. **379**: 1011-1021. Doi: https://doi.org/10.1111/j.1365-2966.2007.11874-.x

[8] Aryal, B., Kafle, P. R. & Saurer, W. 2008. Radial velocity dependence in the spatial orientations of galaxies in and around the local supercluster. *Monthly Notices of the Royal Astronomical Society*. **389**: 741-749. Doi: https://doi.org/10.1111/j.1365-2966.2008.13494-.x

[9] Aryal, B., Neupane, D. & Saurer, W. 2008. Morphological dependence in the spatial orientations of galaxies around the local supercluster. Astrophysics & Space Science, 314, 177-186. Doi: https://doi.org/10.1007/s10509-008-9753-3

[10] Aryal, B., Paudel, S. & Saurer, W. 2008. Coexistence of chiral symmetry restoration and random orientation of galaxies. *Astronomy & Astrophysics*. **479**: 397-407. Doi: https://doi.org/10.1051/0004-6361:20077810

[11] Aryal, B., Bachchan, R. K. & Saurer, W. 2010. Optical search limit and preferred position angles of galaxies in 35 clusters. *Bulletin of the Astronomical Society of India*. **38**: 165-176. Doi: https://doi.org/10.1111/j.1365-2966.2005.09667-.x

[12] Aryal, B., Yadav, S. N. & Saurer, W. 2012. Spatial orientation of galaxies in the Zone of Avoidance. *Bulletin of the Astronomical Society of India*. **40**: 65-76. Doi: https://doi.org/10.1093/mnras/stt1124

[13] Aryal, B., Bhattarai, H., Dhakal, S., Rajbahak, C. & Saurer, W. 2013. Spatial orientation of angular momentum vectors of galaxies in six rotating clusters. *Monthly Notices of the Royal Astronomical Society*. **434**: 1939-1951. Doi: https://doi.org/10.1093/mnras/stt1124

[14] Aryal, B. & Saurer, W. 2000. Comments on the expected isotropic distribution curves in galaxy orientation studies. *Astronomy & Astrophysics*. **364**: L97-111.

[15] Aryal, B. & Saurer, W. 2001. The influence of selection effects on the isotropic distribution curve in galaxy orientation studies. *In Galaxy disks and disk galaxies*. **230**: A145-154.

[16] Aryal, B. & Saurer, W. 2004. Spin vector orientations of galaxies in eight Abell clusters of BM type I. *Astronomy & Astrophysics*. **425**: 871-879. Doi: https://doi.org/10.1051/0004-6361:20041228

[17] Aryal, B. & Saurer, W. 2005a. Spin vector orientations of galaxies in seven Abell clusters of BM type III. *Astronomy & Astrophysics*. **432**: 841-831. Doi: https://doi.org/10.1051/0004-6361:20041975

[18] Aryal, B. & Saurer, W. 2005b. Morphological dependence in the spatial orientations of local supercluster galaxies. *Astronomy & Astrophysics*. **432**: 431-439. Doi: https://doi.org/10.1051/0004-6361:20041679

[19] Aryal, B. & Saurer, W. 2005c. Spin vector orientation of galaxies in the region 15h48m≤(2000)≤19h28m, -68°≤_(2000)≤-62°. *Monthly Notices of the Royal Astronomical Society*. **360**: 125-135. Doi: https://doi.org/10.1111/j.1365-2966.2005.09015-x

[20] Aryal, B. & Saurer, W. 2006. Spatial orientations of galaxies in 10 Abell clusters of BM type II-III. *Monthly Notices of the Royal Astronomical Society*. **366**: 438-449. Doi: https://doi.org/10.1111/j.1365-2966.2005.09667-.x

[21] Flin, P. & Godlowski, W. 1986. The orientation of galaxies in the local supercluster. *Monthly Notices of the Royal Astronomical Society*. **222**: 535-533. Doi: https://doi.org/10.1093/mnras/222.3.525

[22] Yadav, S. N., Aryal, B. & Saurer, W. 2013. Position angle distribution of galaxies in 35 clusters. *Himalayan Physics*. **4**: 1-9. Doi: https://doi.org/10.3126/hj.v4i0.9417

[23] Doroshkevich, A. G. 1973. The origin of rotation of galaxies. *The Astrophysical Journal*. **14**: 11-13.

[24] Doroshkevich, A. G., Shandarin, S. F. & Saar, E. 1978. Spatial structure of protoclusters and the formation of galaxies. *Monthly Notices of the Royal Astronomical Society*. **184**: 643-660. Doi: https://doi.org/10.1093/mnras/184.3.643

[25] Holmberg, E. 1946. On the apparent diameters and the orientation in space of extragalactic nebulae. *Meddelanden fran Lunds Astronomiska Observatorium Series II*. **117**: 3-82.

[26] Ozernoy, L. M. 1971. Dynamical parameters of galaxy clusters as a consequence of cosmological turbulence. *Soviet Astronomy*. **15**: 923-933.

[27] Ozernoy, L.M. 1978. The Whirl Theory of the origin of structure in

the Universe. In: Proceedings of IAU Symposium No. 79, The Large Scale Structure of the Universe. Longair, M.S. and Einasto, J. (eds.). Reidel, Dordrecht. p:427.

[28] Stein, R. 1974. Galaxy formation from primordial turbulence. *Astronomy & Astrophysics*. **35**: 17-29.

[29] Kausch, W. 2004. *A statistical approach to a possible alignment of galaxies in the Perseus Cluster*. M.Sc. thesis. Innsbruck University, Innsbruck, Austria.

[30] Sah, S. S. P. & Yadav, S. N. 2022. Study of preferred alignments of angular momentum vector of i-magnitude SDSS galaxies having redshift 0.54–0.60. *BIBECHANA*. **19**(1-2): 68-74.
Doi: https://doi.org/10.3126/bibechana.v19i1-2.46389

[31] Yadav, S. N. & Sah, S. K. 2021. Study of spatial orientation of angular momentum of z-magnitude SDSS DR-13 galaxies with redshift 0.50 to 0.53. *Journal of Institute of Science and Technology*. **26**(1): 1-7.
Doi: https://doi.org/10.3126/jist.v26i1.37805

[32] Yadav, S. N. 2020. A study of R-magnitude dependence in spatial orientation of spin vectors of SDSS DR-7 galaxies of redshift 0.10< z < 0.11. *Scientific World*. **13**(13): 42-45.
Doi: https://doi.org/10.3126/sw.v13i13.30506

[33] Yadav, S. N. 2016. A study of z-magnitude dependence in the spatial orientation of angular momentum vectors of galaxies having redshift < 30,000 km s^{-1}. *Tribhuvan University Journal*. **30**(2): 195-210.
Doi: https://doi.org/10.3126/tuj.v30i2.25564

[34] Godlowski, W. 1993. Galactic orientation within the local supercluster. *Monthly Notices of the Royal Astronomical Society*. **265**: 874-880.
Doi: https://doi.org/10.1093/mnras/265.4.874

[35] Godlowski, W. 1994. Some aspects of the galactic orientation within the local supercluster. *Monthly Notices of the Royal Astronomical Society*. **271**: 19-30.
Doi: https://doi.org/10.1093/mnras/271.1.19

[36] Yadav, S. N., Saurer, W. & Aryal, B. 2015. A study of co-existence between the Hubble flow and the random alignments of spin vectors of SDSS galaxies. *BIBECHANA*. **12**: 114-127.
Doi: https://doi.org/10.3126/bibechana.v12i0.11787

[37] Yadav, S. N., Aryal, B. & Saurer, W. 2017. Preferred alignments of angular momentum vectors of galaxies in six dynamically unstable Abell clusters. *Research in Astronomy and Astrophysics*. **17**(7): 64-1-10.
Doi: https://doi.org/10.1088/1674-4527/17/7/64

[38] Yadav, S. N. & Aryal, B. 2014. A study of r- and u-magnitude dependence in the spatial orientation of spin vectors of SDSS galaxies having redshift 0.10< z < 0.11. *Himalayan Physics*. **5**: 1-11.
Doi: https://doi.org/10.3126/hj.v5i0.12814